Desalination and Water Treatment
www.deswater.com

doi:10.5004/dwt.2019.24438

164 (2019) 378–387
October

Adsorption and mechanism study for reactive red 120 dye removal by cross-linked chitosan-epichlorohydrin biobeads

Ali H. Jawad[a,*], Nur Shazwani Abdul Mubarak[a], S. Sabar[b]

[a]*Faculty of Applied Sciences, Universiti Teknologi MARA, 40450 Shah Alam, Selangor, Malaysia, Tel. +60355211721, email: ahjm72@gmail.com, ali288@uitm.edu.my (A.H. Jawad), Tel. +60174269877, email: shazwanimubarak@yahoo.com (N.S.A. Mubarak)*
[b]*Chemistry Section, School of Distance Education, Universiti Sains Malaysia, 11800 Minden, Penang, Malaysia, Tel. +6046532284, email: sumiyyahs@usm.my (S. Sabar)*

Received 16 November 2018; Accepted 17 May 2019

ABSTRACT

In this research, cross-linked chitosan-epichlorohydrin biobeads (CEB) were prepared to be potential biosorbent for reactive red 120 (RR120) dye removal from aqueous solution. Adsorption experiments were carried out as a function of contact time (0–600 min), initial dye concentration (30–400 mg/L), and pH (3–12). The adsorption data of RR120 on CEB were in agreement with Langmuir isotherm. The adsorption capacity of CEB for RR120 was 81.3 mg/g at 303 K. The kinetic data were well described by pseudo-second-order kinetic model. The adsorption process was spontaneous and endothermic in nature. The mechanism of adsorption included mainly hydrogen bonding interaction, electrostatic attractions, and n-π stacking interaction. This study reveals that the CEB as a promising biomaterial for removal of reactive dye from aqueous solutions.

Keywords: Chitosan; Cross-linking; Epichlorohydrin; Adsorption; Reactive Red 120; Adsorption mechanism

1. Introduction

Dyes are color bearing organic compounds which are one of the major substrates of the wastewater produced from many industries like textile materials, paper, plastic, osmetics, and etc. Dyes are recalcitrant and stable towards the environment and some of them are also carcinogenic and teratogenic offering significant risk to the aquatic species and human beings [1]. Adsorption is a convenient and well known technique that commonly applied in the removal of dyes compare to other dye treatment methods such as advanced oxidation process, electrochemical destruction, Fenton reaction, oxidation, ozonation, photochemical, ultraviolet irradiation, and adsorption have been established in countless research papers claiming successful dye removal [2]. Activated carbon has been known as a potential adsorbent for removing dyes and various organic and inorganic contaminants from polluted water. However, due to a high operational cost, and extremely difficult for regeneration, and difficulties of adsorbent powder recovery during and at the end of analysis limits its application in huge scale [3].

Chitosan is a well-known cationic polysaccharide and abundantly available low-cost biopolymer. Chitosan is an ideal adsorbent for removal of unlimited numbers of water pollutants and various classes of textile and food dyes [4]. The presence of free amino (–NH_2) and hydroxyl (–OH) groups in the molecular structure of chitosan can effectively serve as active adsorption sites [5]. The protonation of amino groups in acidic media is responsible for increasing the electrostatic attraction towards anionic dyes. However, due to the solubility of raw chitosan in many organic acids and high swelling capacity in water, compressible at high operating pressure, low mechanical strength, and low surface area limit the application of this material in water treatment technologies [6].

Several modifications methods have been made in order to improve the physicochemical properties of chi-

*Corresponding author.

tosan, which generally involved physical modification [7], chemical modification [8], and photo transformation [9]. Chemical cross-linking reaction is one of the convenient and practical ways to improve physical/mechanical properties of chitosan. It is responsible for reducing the degree of swelling and lechabilty of chitosan in aqueous environment, in addition to change the crystalline nature of chitosan and enhance sorption abilities [10]. The cross-linking step is also responsible for reducing the adsorption capacity of chitosan, if amine groups are involved in cross-linking reaction. To date, the widely used cross-linking agents that preferentially bind to the free amino and hydroxyl groups are glutaraldehyde (1,5-pentanodial) and epichlorohydrine (1-cloro-2, 3-epoxipropane), respectively [11]. However, the irreversible cross-linking reaction between a free amine ($-NH_2$) group and a dialdehyde bifunctional cross-linking agent, such as glutaraldehyde, leads to deceased adsorption performances involving a decrease in the content of free amine ($-NH_2$) groups and a decrease in the accessibility to the internal sites or blockage of a number of adsorption sites [8].

Therefore, the objective of this work is to produce chemically modified cross-linked chitosan-epichlorohydrin biobeads (CEB) to be an efficient biosorbent for removal reactive red 120 (RR 120) dye from aqueous solution. Epichlorohydrin was chosen as a convenient base catalyzed crosslinking agent. An advantage of epichlorohydrin is that it does not eliminate the cationic amine ($-NH_2$) from chitosan backbone. RR 120 is an anionic sulfonated reactive azo, non-biodegradable dye with complicated molecular structure was selected as a model pollutant in this study.

2. Materials and methods

2.1. Materials

Chitosan medium molecular weight (68.2% degree of deacetylation) was purchased from Sigma-Aldrich. Epichlorohydrine (≥98% [w/v] aqueous solution) was supplied by Fluka. Reactive red 120 (RR120) was purchased from Sigma-Aldrich (molecular weight: 1469.34 g/mol; molecular formula: $C_{44}H_{24}C_{l2}N_{14}Na_6O_{20}S_6$; λ_{max}: 534 nm).Hydrochloric acid (HCl), Sodium hydroxide (NaOH), and other reagents utilized in this work were all of analytical grade. The stock solution with ultra-pure water was used throughout the experiments.

2.2. Preparation of cross-linked chitosan-epichlorohydrine biobeads (CEB)

2 g of chitosan flakes was dissolved in 90 mL of 5% acetic acid solution. The viscous solution of chitosan was left with vigorous stirring using magnetic bar for 24 h to ensure complete dissolution of chitosan flakes. The resultant viscous solution was taken in a 10 mL glass syringe and added as drops at rate 1 mL/min (done manually) through a 22 gauge needle into 1000 mL of 0.5 M NaOH solution. The entire solution was added through the same syringe and needle by refilling. The beads were left stirring for 24 h and washed with distilled water until reaching a neutral pH value. After that, 85 mL of 0.05 M epichlorohydrinewas added into the wet beads with gentle stirring under heating in water bath at temperature 40°C for 2 h to obtain the ratio of 1:1 (mol chitosan: mol Epichlorohydrine). The cross-linked chitosan-epichlorohydrine bio-beads (CEB) were extensively washed with distilled water and air dried for 24 h. Then, the CEB were ground to constant particle size (< 250 μm) before use. The detailed mechanism of cross-linking process between chitosan and epichlorohydrine is shown Fig. 1.

2.3. Characterization of CEB

Nitrogen adsorption surface area measurement of CEB was carried out at 77 K after drying of sample (200°C, 1 h) using a surface area analyzer (Micromeritics, Model ASAP 2020, USA). The apparent nitrogen surface area was calculated using the BET equation for a pressure range p/p_0 0.995, where the pore size distribution was determined from the adsorption branch using Barrett–Joyner–Halenda (BJH) theory. The surface morphology CEB was examined *via* scanning electron microscope (SEM, Zeiss Supra 40 VP, Germany). In this analysis, appropriate amount on CEB was deposited onto double-sided tape and coated with gold for better resolution prior to scan the sample. Elemental analyses (C, H, N, and S) of the samples were measured by using a CHNSO Analyzer (Flash 2000, Organic Elemental Analyzer, Thermo-scientific,Netherland) where the oxygen content was calculated by difference. The

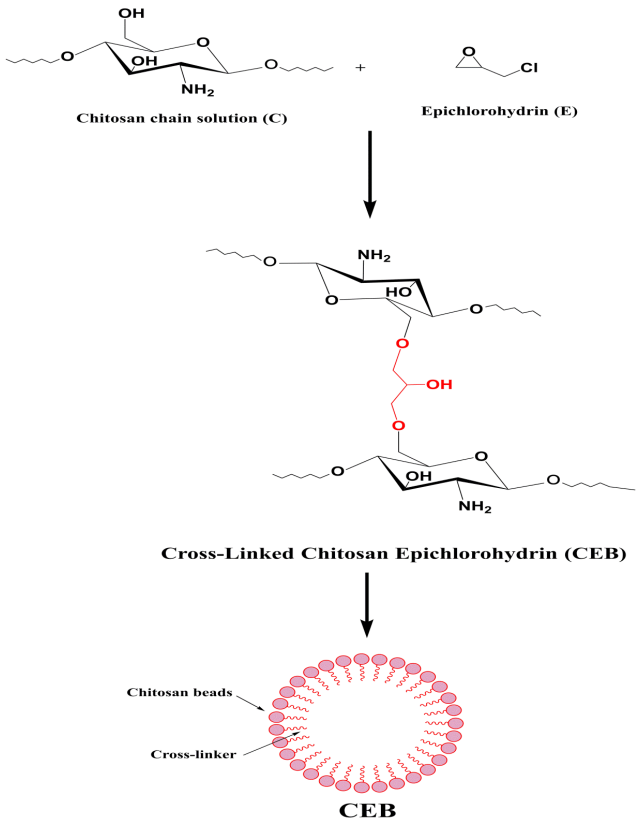

Fig. 1. Crosslinking reaction of chitosan with epichlorohydrine and the molecular structure of their cross-linked biobeads (CEB).

pH-potentiometric titration was performed by the method of Vieira and Beppu [12]. In this method, about 50 mL 0.02 M hydrochloric acid (HCl) was added to 0.1 g of CEB. The aqueous solution of CEB and HCl was left standing for at least 24 h under stirring conditions to protonate CEB. Afterwards, the resulting solution was then titrated against 0.01 M sodium hydroxide solution. The pH of the solution was monitored using a pH meter (Metrohm, 827 pH lab) with a calibrated pH-sensitive glass electrode, where an interval of 2 min was allowed before addition of more NaOH. The amino group composition of CEB was quantitatively determined using Eq. (1).

$$\%NH_2 = \left[\frac{M_{NaOH}(V_2 - V_1)\times 161}{W_2}\right]\times 100 \quad (1)$$

M_{NaOH} was the molarity of the sodium hydroxide (NaOH) solution (M), V_1 and V_2 were the volume (L) of NaOH used to neutralize the excess HCl and the protonated CEB, 161 is the average molecular weight of the chitosan monomer and W_2 was the mass (g) of CEB in its dried form before the potentiometric titration. The two equivalence points on the titration curves were calculated by the derivative method, where the volume difference between these two equivalence points correspond to the acid consumed by the amino (–NH_2) groups. This allows the determination of the content (%) of amino groups in sample according to Eq. (1). The surface charge (pHpzc) was measured by using the pH drift method with a pH meter (Metrohm, 827 pH lab). In this experiment, pH was adjusted to a series of initial values between 2 and 12 by adding either HCl or NaOH and then CEB (0.15 g) to the solution. These were then shaken for 24 h in an isothermal water bath shaker, a revolving water bath to reach equilibrium, after which each resulting pH was measured and the initial pH (pH_o) versus the difference between the initial and final pH values (ΔpH) was plotted. The pzc was taken as the point where ΔpH = 0. The functional groups of CEB before and after RR120 adsorption were identified by Fourier Transform Infrared (FTIR) Spectroscopy (Perkin-Elmer, Spectrum RX I).

2.4. Batch equilibrium studies

The adsorption of RR120 on CEB was investigated in a batch mode. The experiments were performed in a series of 250 mL Erlenmeyer flask containing 100 mL of RR120 solution with different initial RR120 concentrations (30–400 mg/L). The dosage of CEB ranging from 0.02 to 1.2 g in 100 mL were added to the RR120 solution with pH varied from pH 3–12 and agitated with fixed shaking speed of 110 strokes/min at 303 K by using a thermostat shaker (Memmertwaterbath model WNB7-45, Germany). After the stirring, the supernatant was collected with a 0.20 μm Nylon syringe filter and the concentrations of RR120 were monitored at a different time interval using a HACH DR 2800 Direct Reading Spectrophotometer at a wavelength of 534 nm. The effect of temperature on RR120 uptake was performed by following the same procedures at 303K, 313K and 323 K. The adsorption capacity at equilibrium, q_e (mg/g) and the percent of dye removal (DR (%)) of studied dyes were determined using Eqs. (2) and (3) respectively.

$$q_e = \frac{(C_o - C_e)V}{W} \quad (2)$$

$$DR\,\% = \frac{(C_o - C_e)}{C_o}\times 100 \quad (3)$$

where C_o: Initial concentrations of the RR120 (mg/L); C_e: Liquid-phase concentrations of the RR120 (mg/L) at equilibrium; V: Volume of the RR120 solution (L); W: The dried weight of CEB (g)

3. Results and discussion

3.1. Characterization of CEB

3.1.1. Surface area analysis

BET surface area of CEB was measured and given in Table 1. Result shows that CEB has a low surface area of 0.70 (m^2/g), whereas the decrease in total pore volume reflects the increase of adsorbent density [13]. The classification of pore size by International Union of Pure and Applied Chemistry (IUPAC) indicates that CEB consists of mesopores (pore diameter range: 2–50 nm). In fact, cross-linking reaction is responsible for producing compact, dense adsorbent with significantly lower surface area with relatively pore diameter.

3.1.2. Elemental analysis

The elemental analysis (CHN) result of the CEB is given in Table 1. It was found that content carbon, hydrogen, and nitrogen content is quite comparable to the unmodified chitosan [6], and the changes in the elements content were minor at the best. This observation indicates that the cross-linking reaction with epichlorohydrine did not altering much the molecular structure of CEB.

3.1.3. pH-potentiometric titration

The potentiometric titration test was carried out in order to quantitatively determine the actual content (%) of amino groups in the polymeric structure of CEB. Furthermore, it can also provide useful information about the

Table 1
The physicochemical properties of CEB

Analysis	Value
Textural properties	
BET surface area (m^2/g)	0.70
Mean pore diameter (nm)	6.50
Elemental analysis (wt. %)	
C	38.92
H	6.91
N	7.03
O (by difference)	47.14
pH-Potentiometric titration, -NH_2 (%)	53.1±2.0

available amino (-NH_2) on the polymeric matrix of the CEB after cross-linking reaction, which can serve as active sides in the adsorption process. Thus, the typical pH-potentiometric curves, and the individual first derivative curve of the CEB are shown in Fig. 2a and Fig. 2b, respectively. The result obtained from Fig. 2 indicates that the CEB has a relatively high content (53.1%) of free amino (-NH_2) groups in its molecular structure (Table 1).

3.1.4. FTIR spectra

FTIR spectral analysis of CEB before adsorption (Fig. 3a), after RR120 adsorption (Fig. 3b) was carried out. From Fig. 3a, the characteristic bands of CEB shown at ~3421cm^{-1} (O-H and N-H stretching vibration), ~2906 cm^{-1} (C-H stretching vibrations in –CH and –CH_2) [5]. A band at ~1654 cm^{-1} (characteristic of amide group, amide I). A band at ~1550 cm^{-1} (-NH_2 bending vibration). Other bands at~1420 cm^{-1} (-NH_2 bending vibration of the primary amino group), ~1368 cm^{-1} (-CH_3 symmetric deformation), ~1320 cm^{-1} (C-N stretching vibration), and ~1073 cm^{-1} (C-O-C stretching vibration of pyranose ring) [5–8]. After RR120 adsorption (Fig. 3b), a prominent band around 2250 cm^{-1} caused by the CN triple bond, in addition to obvious variation in other bands at ~ 1550 cm^{-1}, 1368 cm^{-1}, and 1073 cm^{-1}, which may indicate the possible interaction between the RR120 dye molecules and the available functional groups on the CEB surface.

3.1.5. SEM analysis

SEM analysis was carried out to examine the surface morphology of the CEB before and after adsorption as shown in Fig. 4a and Fig. 4b, respectively. From Fig. 4a indicates the surface of CEB before adsorption was irregular, uneven with heterogeneous cavities that well-distributed across the CEB surface. Therefore, the SEM image indicates that RR120 may be adsorbed on the surface of CEB and the accessible cavities can enhance the RR120 uptake. The surface morphology of CEB after RR120 adsorption reveals a change in the topography of the adsorbent, as evidenced by compact surface with less cavities and wavy surface features due to RR120 loaded onto CEB surface (Fig. 4b).

3.2. Batch adsorption study

3.2.1. Effect of CEB dosage

The effect of CEB mass on the removal of the RR120 from aqueous solution was carried out by using variable quantities (0.020 to 1.20 g) of CEB at fixed volumes (100 mL) and initial RR120 dye concentration of 100 mg L^{-1}. For this experiment, other operation parameters were kept constant at 303 K, shaking speed of 110 stroke min^{-1}, contact time of 180 min, and an unadjusted pH at 5.22 for the initial RR120 solution. The results are shown in Fig. 5. It was found that by increasing the mass of CEB till 0.5 g the removal percentage increased rapidly and further addition was not significantly affected the RR120 removal percentage. The observed increase in the RR120 removal (%) with CEB mass was attributed to an increase in the available adsorbent surface area, as the number of adsorption sites increase as well. However, no significant changes in RR120 removal efficiency were observed beyond 0.5 g of CEB dose. Therefore, 0.5 g of CEB was selected for subsequent work.

3.2.2. Effect of solution pH

The acidity of the medium is one of the most significant parameters in adsorption. Therefore, effect of initial solution pH on the RR120 removal was evaluated within pH range between 3–12 as shown in Fig. 6a. It was evident that

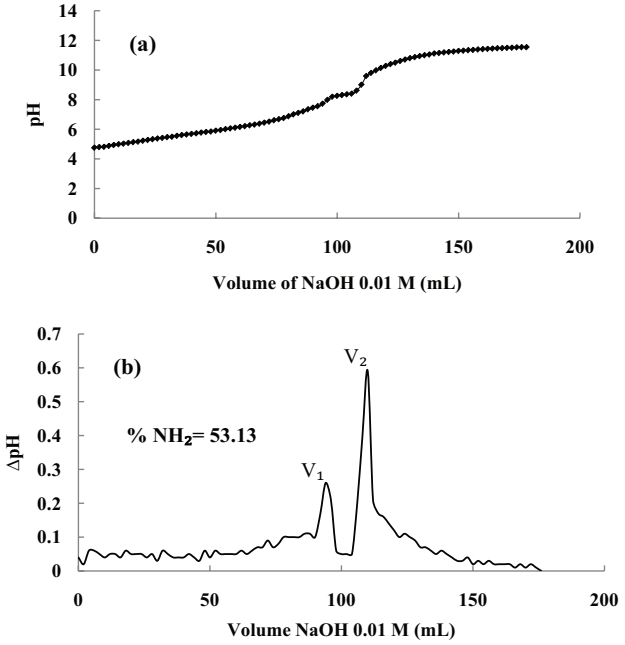

Fig. 2. (a) pH-potentiometric titration curves of CEB, and (b) first order derivative plot based on pH-potentiometric titration curve of CEB.

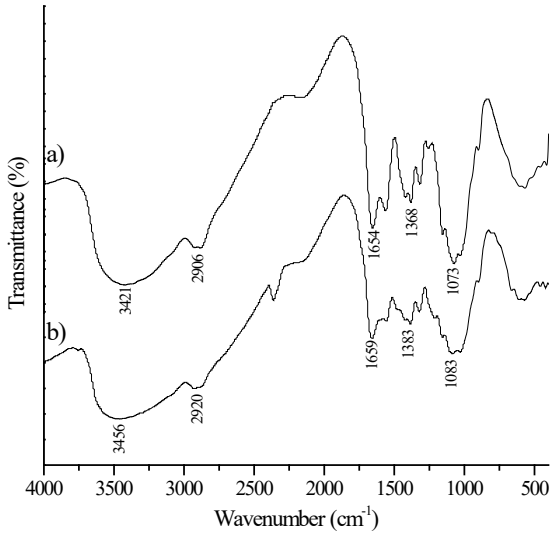

Fig. 3. FTIR spectral analysis of (a) CEB before adsorption, and (b) CEB after RR120 adsorption.

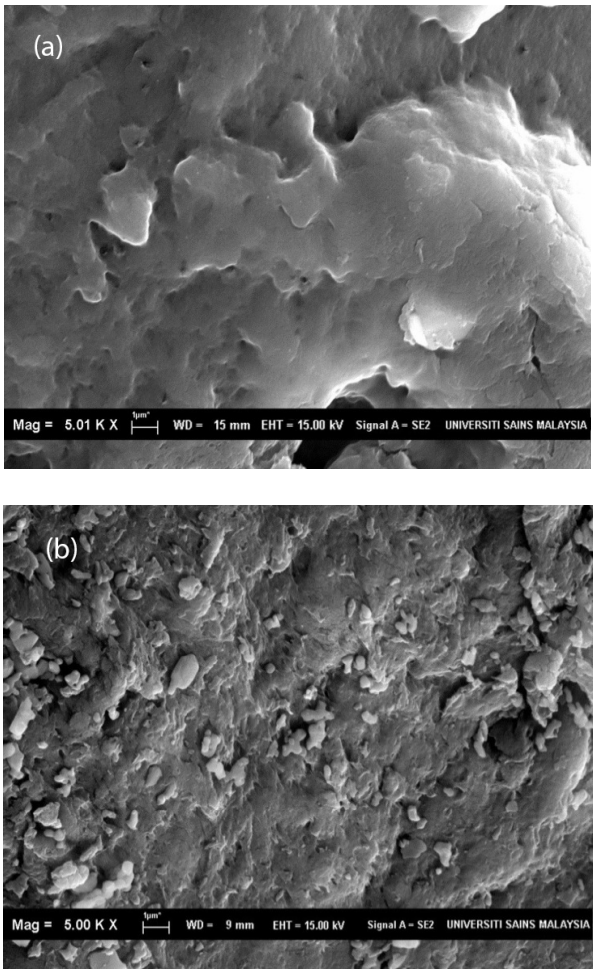

Fig. 4. SEM micrograph of CEB particle (5000× magnification): (a) before adsorption, and (b) after RR120 adsorption.

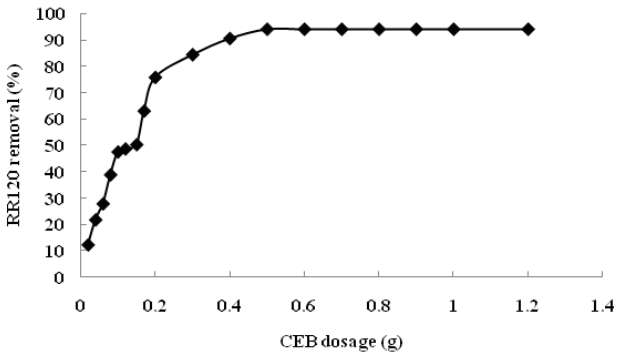

Fig. 5. The effect of CEB mass on the RR120 removal (%) at $[RR120]_o$ = 100 mg L^{-1}, V = 100 mL, unadjusted pH = 5.22, T = 303 K, shaking speed = 110 stroke min^{-1}, and contact time = 180 min.

the maximum RR120 removal was observed at pH 3, and gradual decreases in the RR120 removal can be observed by increasing the pH value towards basic environment. The pH_{pzc} value for the CEB was to be 6.8 Fig. 6b.

This observation indicates the cationic acid character of CEB and reconfirmed the availability of the cationic functional groups on the surface of CEB according to the previously discussed results in potentiometric titration test. A positive charge of CEB can be obtained at pH environment below the pH_{PZC}, preferring the adsorption of negatively charged species such as RR120. For pH values lower than pHpzc, the surface of CEB will be positively charged due to the protonation of amine groups (–NH_2) on the surface of CEB [4,5,7,13]. In fact, protonation process of the CEB is responsible for producing more cationic amines groups on the surface of protonated CEB as shown in Eq. (4):

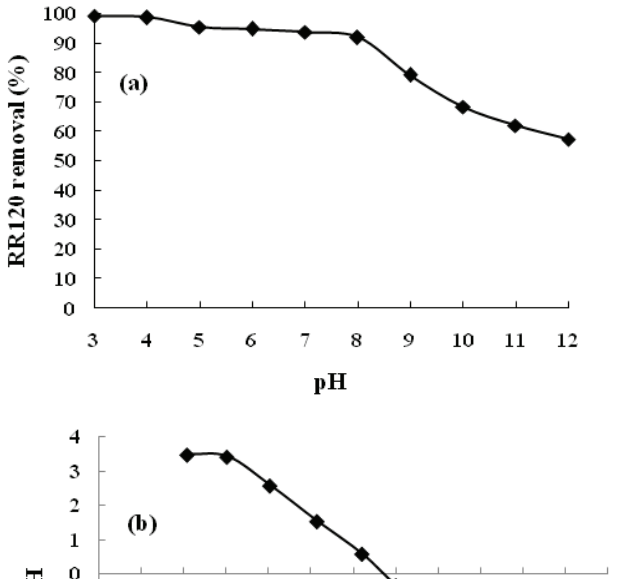

Fig. 6. (a) Effect of solution pH on RR120 dye removal (%) at $[RR120]_o$ = 100 mg/L, V = 100 mL, T = 303 K, stirring speed = 110 rpm, and contact time = 180 min, (b) pH_{PZC} of CEB.

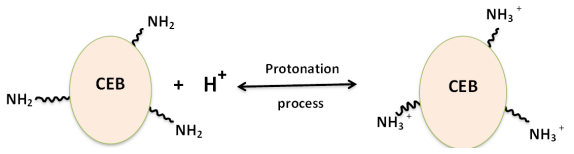

(4)

On the other hand, the sulfonate group (-SO_3H) in the molecular structure of the can be converted in aqueous medium into active negative sulfonate group (-SO_3^-) as shown in Eq. (5).

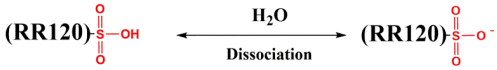

(5)

Consequently, a strong electrostatic (columbic) attraction between positively charged protonated amino groups

of CEB with negatively charged sulfonate group of RR120, and thus increases RR120 adsorption as shown in Eq. (6).

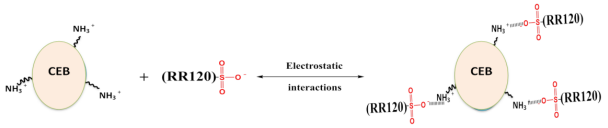

(6)

Moreover, the decreasing in the RR120 removal with increasing pH value can be attributed to the competition between anionic dye and excess OH^- ions in the solution. Therefore, the initial pH ~ 3 of the RR120 solution was selected for further studies.

3.2.3. Effect of C_o and contact time

The influence of contact time and initial RR120 concentration (30–400 mg/L) on the adsorption capacity of CEB is shown in Fig. 7. The experimental data reveal that the adsorption capacity at equilibrium increases from 5.4 to 74.3 mg/g, with increase in the initial RR120 concentration from 30 to 400 mg/L. This was attributed to a greater collision rate between RR120 molecules and CEB by increasing the initial RR120 concentration. Furthermore, the time to reach equilibrium also increased with the increase in initial RR120 concentration. High uptake at higher initial concentrations may occur because of the formation of driving force by the mass gradient between solutions and the adsorbent that leads to the high amounts of RR120 molecules being transferred to the CEB surface.

3.3. Kinetic studies

The pseudo-first-order model and pseudo-second-order model were used to investigate the adsorption kinetics of RR120 dye on CBE. The conformity between experimental data and the model predicted values was expressed by correlation coefficient (R^2). The pseudo-first-order rate model of Lagergren [14] is based on solid capacity and generally expressed in Eq. (7):

$$\ln(q_e - q) = \ln(q_e) - (k_1)t \tag{7}$$

where q_e is the amount of solute adsorbed at equilibrium per unit weight of adsorbent (mg/g), q is the amount of solute adsorbed at any time (mg/g), and k_1 is the adsorption constant. This expression is the most popular form of pseudo-first-order kinetic model. k_1 values at different initial MB concentrations were calculated from the plots of $\ln(q_e - q)$ versus t. Constant k_1 and correlation coefficients (R^2) were calculated and summarized (Table 2). The correlation coefficient (R^2) values obtained were relatively low; hence, this model has very poor correlation coefficients (R^2) for the best fit data. Furthermore, the kinetic data were analyzed using the pseudo-second-order model [15], which can be expressed in Eq. (8):

$$\frac{t}{q} = \left(\frac{1}{k_2 q_e^2}\right) + \left(\frac{1}{q_e}\right)t \tag{8}$$

The plot of t/q versus t should give a linear relationship, from which q_e and k_2 can be determined from the slope and intercept of the plot. The k_2 and q_e determined from the model along with the corresponding correlation coefficient (R^2) values are presented in Table 2. The values of the calculated and experimental q_e are also presented in Table 2. Based on the given data, the adsorption of RR120 dye perfectly followed the pseudo-second-order kinetic model.

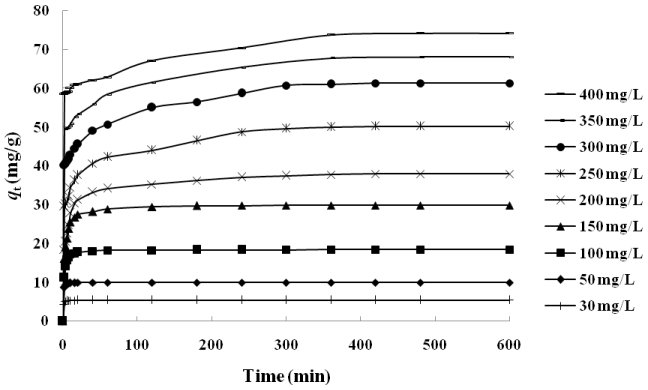

Fig. 7. Effect of contact time and initial concentration on the adsorption of RR120 on CEB (V = 250 mL, T = 303 K, stirring speed = 110 rpm, CEB dosage = 0.5, and pH = 3.

3.4. Isotherm modeling

To quantify the adsorption capacity of CEB for the removal of RR120 dye from aqueous solutions, we tested the Langmuir, Freundlich, and Temkin isotherm models. The Langmuir model assumes that the adsorptions occur at specific homogeneous sites on the adsorbent. This model is successfully used in numerous monolayer adsorption processes [16]. The data of the equilibrium studies for the adsorption of RR120 dye onto CEB may follow the Langmuir model as given in Eq. (9):

$$\frac{C_e}{q_e} = \frac{1}{q_m K_L} + \frac{1}{q_m} C_e \tag{9}$$

where C_e is the equilibrium concentration (mg/L) and q_e is the amount adsorbed per specified amount of adsorbent (mg/g), K_L is the Langmuir equilibrium constant, and q_m is the amount of adsorbate required to form a monolayer. Hence, a plot of C_e/q_e vs. C_e should be a straight line with a slope $(1/q_m)$ and an intercept as $(1/q_m K_L)$ (Fig. 8a). The Langmuir type adsorption isotherm indicates the surface homogeneity of the adsorbent. The adsorbent surface is made up of small adsorption patches, which are energetically equivalent to each other in terms of adsorption phenomenon. The correlation coefficient (R^2) ≥ 0.99 revealed that the adsorption data of RR120 dye on CEB well fitted to the Langmuir isotherm. The values of constants K_L and b were calculated and the results are shown in Table 3.

The essential characteristics of Langmuir isotherm can be expressed in terms of separation factor R_L, a dimensionless constant [17], which is given in Eq. (10):

$$R_L = \frac{1}{(1 + K_L C_0)} \tag{10}$$

Table 2
Kinetic parameters values for adsorption of RR120 on CEB

[RR120] (mg/L)	$q_{e,Exp.}$ (mg/g)	Pseudo-first-order model			Pseudo-second-order		
		$q_{e.Cal.}$ (mg/g)	k_1 (min^{-1})×10^{-2}	R^2	$q_{e.Cal.}$ (mg/g)	k_2 (g/mg min)×10^{-2}	R^2
30	5.4	1.3	24.4	0.80	5.4	155	1.0
50	9.9	6.7	13.7	0.72	9.6	86	1.0
100	18.5	8.6	27.8	0.73	17.6	61	1.0
150	29.8	13.7	28.1	0.87	30.6	18	1.0
200	37.9	14.1	17.2	0.81	38.2	5.5	0.99
250	50.3	21.0	12.6	0.93	50.7	2.9	0.99
300	61.4	25.4	12.7	0.88	61.9	2.4	0.99
350	70.2	31.5	6.6	0.80	70.1	2.2	0.99
400	77.4	39.9	5.1	0.77	78.8	1.7	0.99

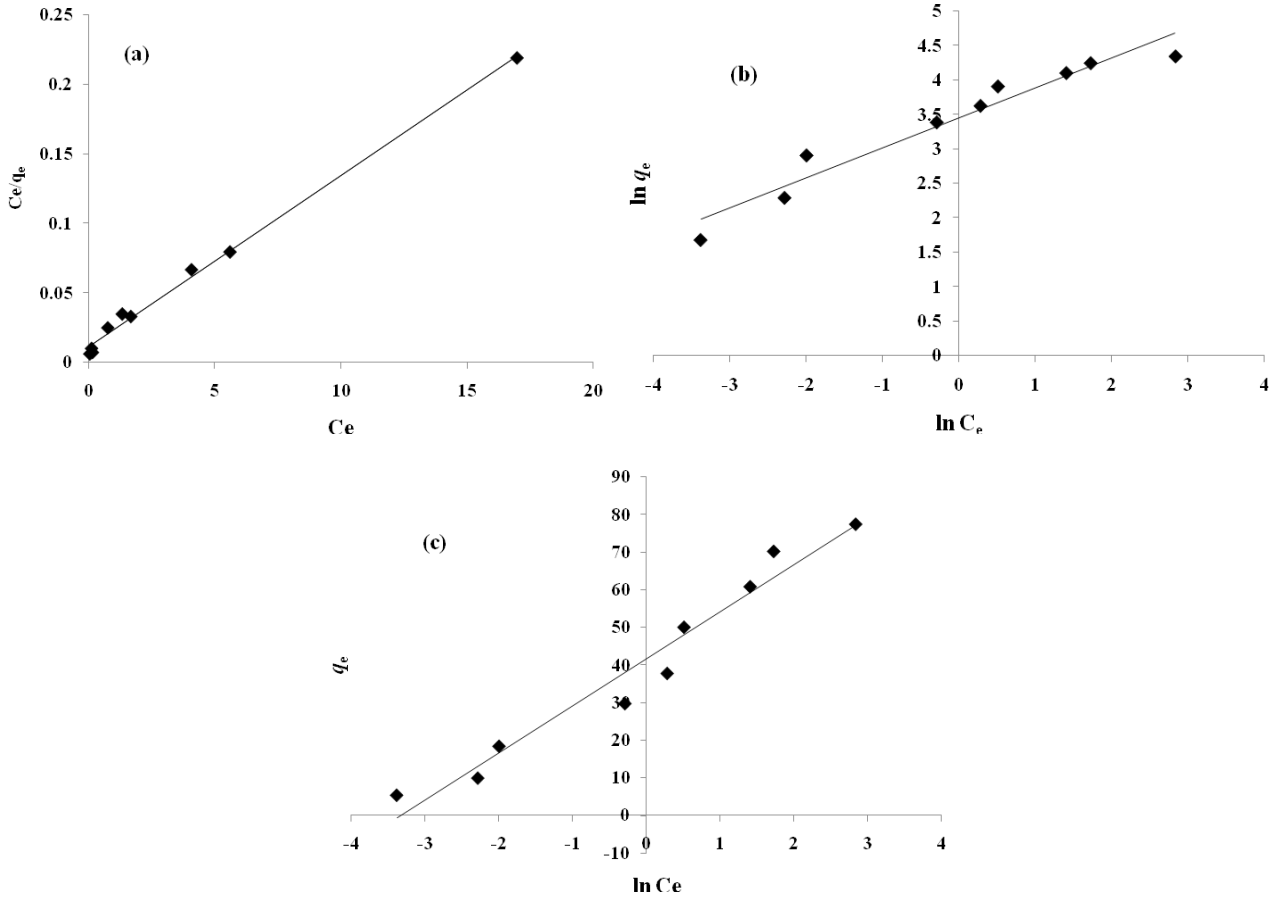

Fig. 8. Isotherm for the adsorption of RR120 dye on CEB at 303K: (a) Langmuir, (b) Freundlich, and (c) Temkin.

An adsorption system is considered favorable when $0 < R_L < 1$, unfavorable when $R_L > 1$, linear when $R_L = 1$, or irreversible when $R_L = 0$. In this study, the values of R_L obtained were between 0 and 1. Therefore, the adsorption process is favorable. The calculated R_L values at different initial MB concentrations are shown in Fig. 9. The R_L value, which was within the range of 0–1 at all initial dye concentrations, confirms the favorable uptake of RR120 over the entire range of concentration levels.

Moreover, the Freundlich model can be applied for non-ideal adsorption on heterogeneous surfaces and multilayer adsorption [18]. This model is presented in Eq. (11).

$$\ln q_e = \ln K_F + \frac{1}{n}\ln C_e \tag{11}$$

where K_F is the Freundlich equilibrium constant, n is an empirical constant, and the rest of the terms have the usual

Table 3
Parameters of the Langmuir, Freundlich and Temkin isotherm models for RR120 adsorption on CEB at 303K

Adsorption isotherms	Value
Langmuir	
q_m (mg/g)	81.3
K_L (L/mg)	1.05
R^2	0.99
Freundlich	
K_F (mg/g)	31.6
n	2.3
R^2	0.94
Temkin	
K_T (L/mg)	1.20
B (J/mol)	12.5
R^2	0.95

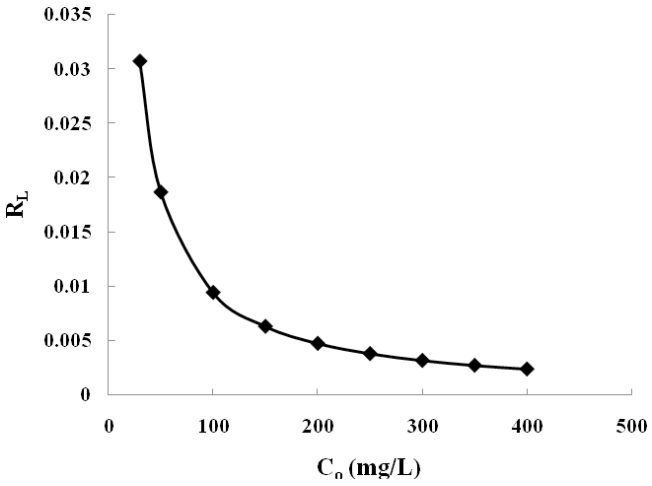

Fig. 9. Values of R_L for the adsorption of the RR120 on CEB at different initial RR120 concentrations.

significance. Thus, a plot of ln q_e vs. ln C_e should be a straight line with a slope $1/n$ and an intercept of ln K_F (Fig. 7b). The related parameters were calculated, and the results are shown in Table 3.

Temkin and Pyzhev [19] considered the effects of indirect adsorbate/adsorbate interactions on adsorption isotherms. The Temkin isotherm equation can be expressed in Eq. (13).

$$q_e = B\ lnK_T + B\ lnC_e \quad (13)$$

where $B = (RT/b)$, a plot of q_e versus lnC_e yielded a linear line (Fig. 7c), enables to determine the isotherm constants K_T and B. K_T is the Temkin equilibrium binding constant (L/mg) that corresponds to the maximum binding energy, and constant B is related to adsorption heat. The adsorption heat of all the molecules in the layer is expected to decrease linearly with coverage because of adsorbate/adsorbate interactions. The constants K_T and B as well as the R^2 values are shown in Table 3. The Langmuir model fit the data better than the Freundlich and Temkin models (Figs. 7a, 7b, 7c and Table 3). This result is also confirmed by the high R^2 value for the Langmuir model (0.99) compared with the Freundlich (0.94) and Temkin (0.95) models. Therefore, the adsorption of RR120 on CEB occurs as monolayer adsorption on a surface that is homogenous in adsorption affinity. The computed maximum monolayer adsorption capacity (q_m) of CEB for RR120 was 81.3 mg/g (Table 3). The maximum sorption capacity (q_m) of the CEB adsorbent for RR120 was compared with those reported in literature for different adsorbents/RR120 adsorption systems (Table 4).

Table 4
Adsorption capacities for RR120 by various adsorbents

Adsorbent	Adsorption capacity (mg/g)	pH	Reference
CEB	81.3	3	This study
Spirogyra majuscula	722.4	3	[20]
Spirogyra majuscula	333	2	[20]
Heat-treated-fungal biomass	182.9	3	[21]
Nanoparticles of Fe_3O_4	166.6	2.5	[22]
Spirogyra majuscula	156	4	[20]
Acid-treated- fungal biomass	138.6	3	[21]
Spirogyra majuscula	123.1	5	[20]
Native- fungal biomass	117.8	3	[21]
Cetylpyridinium modified resadiye bentonite	81.9	6.7	[23]
Base-treated- fungal biomass	57.2	3	[21]
4-(2-pyridylazo) resorcinol	49.26	2.5	[22]
Chitosan–octadecylamine	5.6	5	[24]

3.5. Adsorption mechanism

The proposed adsorption mechanism of RR120 on CEB is sketched in Fig. 10. According to the available functional groups on the surface of CEB, the adsorption mechanism of RR120 on CEB can be assigned to the various interactions, e.g., hydrogen bonding interaction (Fig. 10a), electrostatic attractions (Fig. 10b), and n-π stacking interaction (Fig. 10c). Similar observation was reported by Azha et al., [25] for adsorption of Acid Red 1 dye on the surface of the amphoteric adsorbent. In fact, the electrostatic interaction between negatively charged sulfonate (SO_3^-) acid group of RR120 and the positively charged CEB improved the adsorption. RR120 contains hexa-sulfonate (SO_3^-) acid groups in its molecular structure, resulting in more uptake of RR120 by the CEB (Fig. 10b). In this respect, Heibati et al. [26] attributed the possible adsorption mechanism of Reactive Black 5 by pumice and walnut activated carbon to the electrostatic attractions between positively charged adsorbents and negatively charged adsorbate. Another important factor for RR120

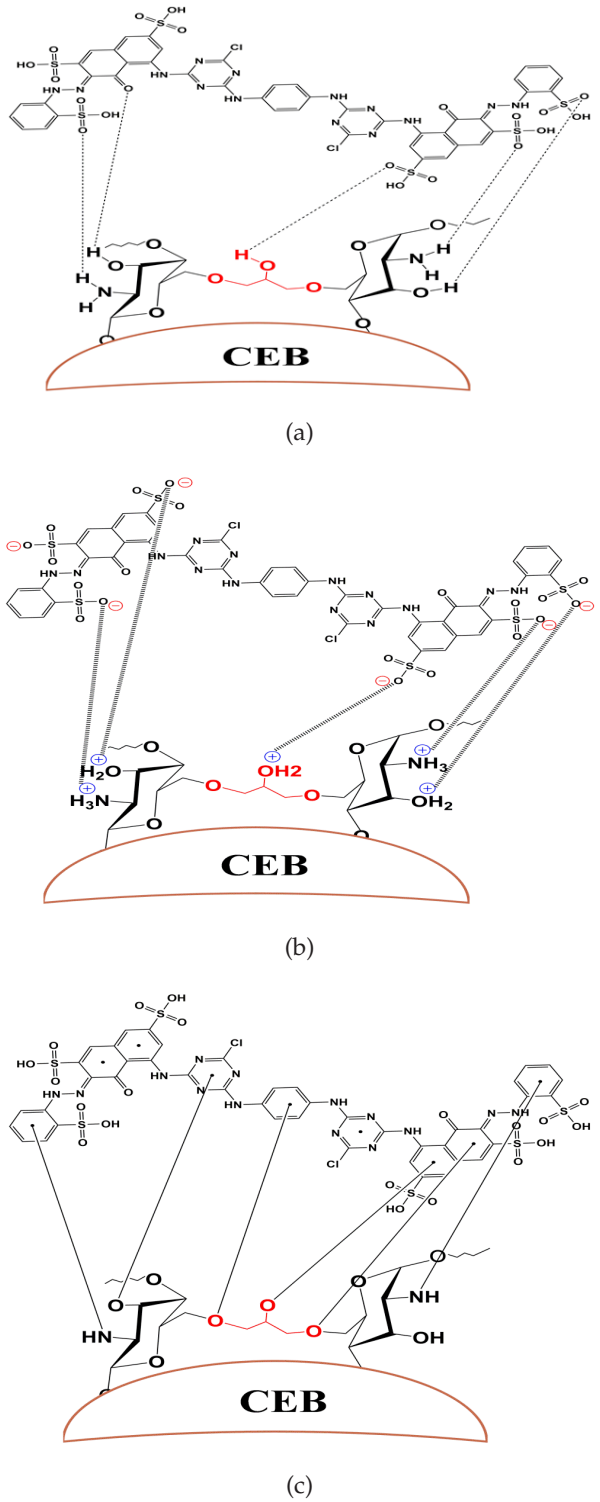

Fig. 10. Possible mechanism of various types of interactions between RR120 with CEB: (a) hydrogen bonding, (b) electrostatic bonding, and (c) n–π interactions.

adsorption on CEB is the *n*-π stacking interaction (Fig. 10c). In fact, the *n*–π interaction is generally occurred where the lone pair electrons on an oxygen atom are delocalized into the π orbital of an aromatic ring of dyes [27].

Table 5
Thermodynamic parameters for the adsorption of RR120 on CEB

T (K)	$ln\ k_d$	ΔG°_{ads} (kJ mol^{-1})	ΔH°_{ads} (kJ mol^{-1})	ΔS°_{ads} (J mol^{-1})
303	2.6	–2.4	27.7	0.099
313	3.7	–3.3		
323	5.3	–4.22		

3.6. Adsorption thermodynamics

Adsorption thermodynamics of RR120 on CEB were determined form the experimental data obtained at various temperatures of 303 K, 313 K, and 323 K and the thermodynamic parameters, such as Gibb's free energy (ΔG°), enthalpy (ΔH°) and entropy (ΔS°) were calculated using the following Eqs. (14–16) [28]:

$$k_d = \frac{q_e}{C_e} \tag{14}$$

$$\Delta G^\circ = \Delta H^\circ - T\Delta S^\circ \tag{15}$$

$$\ln k_d = \frac{\Delta S^\circ}{R} - \frac{\Delta H^\circ}{RT} \tag{16}$$

where q_e is the RR120 concentration adsorbed on CEB at equilibrium (mg/L), C_e is the equilibrium RR120 concentration in the liquid phase (mg/L), and k_d is the distribution coefficient, R is the universal gas constant (8.314J/mol·K) and T is the absolute temperature (K). The values of ΔH° and ΔS° were calculated from the slope and intercept of van't Hoff plots of $ln\ k_d$ versus $1/T$ respectively. The thermodynamic parameters are listed in Table 5. The negative values of ΔG° indicate the adsorption of RR120 on CEB was spontaneous and more favorable at high temperature [29]. The positive value of the enthalpy change (ΔH°) indicates that the adsorption process is an endothermic in nature. The positive entropy change (ΔS°) value corresponds to the increase in the randomness at solid-solution interface.

4. Conclusion

Cross-linked chitosan-epichlorohydrine bio-beads (CEB) were synthesized in this work to be biosorbent for RR120 removal from aqueous solutions. Optimum adsorption conditions of RR120 were found at adsorbent dosage of 0.5 g/100 mL, and pH 3, and with maximum adsorption capacity of 81.3 mg/g. The Langmuir model was found to fit well with the experimental data. The kinetic data of the RR120 adsorption under all studied initial concentrations fitted well with the pseudo-second-order kinetic model. Thermodynamic functions show a spontaneous and endothermic nature of the adsorption process. The mechanism of adsorption included mainly hydrogen bonding interaction, electrostatic attractions, and n-π stacking interaction. Thus, CEB can be considered a potential biosorbent for removal of acid reactive form aqueous solution.

References

[1] A.H. Jawad, R.A. Rashid, K. Ismail, S. Sabar, High surface area mesoporous activated carbon developed from coconut leaf by chemical activation with H_3PO_4 for adsorption of methylene blue, Desal. Water Treat., 74 (2017) 326–335.

[2] V. Katheresan, J. Kansedo, S.Y. Lau, Efficiency of various recent wastewater dye removal methods: A review, J. Environ. Chem. Eng., 6(4) (2018) 4676–4697.

[3] R.A. Rashid, A.H. Jawad, M.A.M. Ishak, N.N. Kasim, KOH-activated carbon developed from biomass waste: adsorption equilibrium, kinetic and thermodynamic studies for Methylene blue uptake, Desal. Water Treat., 57(56) (2016) 27226–27236.

[4] A.H. Jawad, N.F.H. Mamat, B.H. Hameed, K. Ismail, Biofilm of cross-linked chitosan-ethylene glycol diglycidylether for removal of reactive red 120 and methyl orange: adsorption and mechanism studies, J. Environ. Chem. Eng., 7(2) (2019) 102965.

[5] A.H. Jawad, M.A. Islam, B.H. Hameed, Cross-linked chitosan thin film coated onto glass plate as an effective adsorbent for adsorption of reactive orange 16, Int. J. Biol. Macromol., 95 (2017) 743–749.

[6] M.N. Nawi, A.H. Jawad, S. Sabar, W.S.W. Ngah, Photocatalytic-oxidation of solid state chitosan by immobilized bilayer assembly of TiO_2-chitosan under a compact household fluorescent lamp irradiation, Carbohydr. Polym., 83 (2011) 1146–1152.

[7] N.S.A. Mubarak, A.H. Jawad, W.I. Nawawi, Equilibrium, kinetic and thermodynamic studies of Reactive Red 120 dye adsorption by chitosan beads from aqueous solution, Ener., Ecolo., Environ., 2(1) (2017) 85–93.

[8] A.H. Jawad, M.A. Nawi, Characterizations of the photocatalytically-oxidized cross-linked chitosan-glutaraldehyde and its application as a sub-layer in the TiO_2/CS-GLA bilayer photocatalyst system, J. Polym. Environ., 20 (2012) 817–829.

[9] A.H. Jawad, M.A. Nawi, M.H. Mohamed, L.D. Wilson, Oxidation of chitosan in solution by photocatalysis and product characterization, J. Polym. Environ., 25(3) (2017) 828–835.

[10] Y. Wan, K.A. Creber, B. Peppley, V.T. Bui, Ionic conductivity and related properties of crosslinked chitosan membranes, J. Appl. Polym. Sci., 89(2) (2003) 306–317.

[11] W.S.W. Ngah, C.S. Endud, R. Mayanar, Removal of copper (II) ions from aqueous solution onto chitosan and cross-linked chitosan beads, React. Funct. Polym., 50 (2002) 181–190.

[12] R.S. Vieira, M.M. Beppu, Interaction of natural and crosslinked chitosan membranes with Hg (II) ions, Colloids Surf. A Physicochem. Eng. Asp., 279 (2006) 196–207.

[13] M.A. Nawi, S. Sabar, A.H. Jawad, Sheilatina, W.S.W. Ngah, Adsorption of Reactive Red 4 by immobilized chitosan on glass plates: Towards the design of immobilized TiO_2-chitosan synergistic photocatalyst-adsorption bilayer system, Biochem. Eng. J., 49 (2010) 317–325.

[14] S. Lagergren, Zurtheorie der sogenannten adsorption gelosterstoffe. Kungliga svenskavetenskapsakademiens, Handlingar, 24 (1898) 1–39.

[15] Y.S. Ho, G. McKay, Sorption of dye from aqueous solution by peat, Chem. Eng. J., 70(2) (1998) 115–124.

[16] I. Langmuir, The adsorption of gases on plane surfaces of glass, mica and platinum, J. Am. Chem. Soc., 40(9) (1918) 1361–1403.

[17] K.R. Hall, L.C. Eagleton, A. Acrivos, T. Vermeulen, Pore- and solid-diffusion kinetics in fixed-bed adsorption under constant-pattern conditions, Ind. Eng. Chem. Fundam., 5 (1966) 212–223.

[18] H.M.F. Freundlich, Over the adsorption in solution, J. Phys. Chem., 57 (1906) 385–471.

[19] M.I. Temkin, V. Pyzhev, Kinetics of ammonia synthesis on promoted iron catalyst, Acta Phys. Chim. USSR, 12(1) (1940) 217–222.

[20] A. Celekli, M. Yavuzatmaca, H. Bozkurt, Kinetic and equilibrium studies on the adsorption of reactive red 120 from aqueous solution on *Spirogyra majuscule*, Chem. Eng. J., 152 (2009) 139–145.

[21] M.Y. Arıca, G. Bayramoglu, Biosorption of reactive Red-120 dye from aqueous solution by native and modified fungus biomass preparations, J. Hazard. Mater., 149 (2007) 499–507.

[22] G. Absalan, M. Asadi, S. Kamran, L. Sheikhian, D.M. Goltz, Removal of reactive red-120 and 4-(2-pyridylazo) resorcinol from aqueous samples by Fe_3O_4 magnetic nanoparticles using ionic liquid as modifier, J. Hazard. Mater., 192 (2011) 476–484.

[23] A. Tabak, N. Baltas, B. Afsin, M. Emirik, B. Caglar, E. Erend, Adsorption of reactive Red 120 from aqueous solutions by cetylpyridinium-bentonite, J. Chem. Technol. Biotechnol., 85 (2010) 1199–1207.

[24] S. Kittinaovarat, P. Kansomwan, N. Jiratumnukul, Chitosan/modified montmorillonite beads and adsorption Reactive Red 120, Appl. Clay Sci., 48 (2010) 87–91.

[25] S.F. Azha, L. Sellaoui, M.S. Shamsudin, S. Ismail, A. Bonilla-Petriciolet, A.B. Lamine, A. Erto, Synthesis and characterization of a novel amphoteric adsorbent coating for anionic and cationic dyes adsorption: Experimental investigation and statistical physics modelling, Chem. Eng. J., 351 (2018) 221–229.

[26] B. Heibati, S. Rodriguez-Couto, A. Amrane, M. Rafatullah, A. Hawari, M.A. Al-Ghouti, Uptake of reactive Black 5 by pumice and walnut activated carbon: chemistry and adsorption mechanisms, J. Ind. Eng. Chem., 20(5) (2014) 2939–2947.

[27] A.T. Mohammad, A.S. Abdulhameed, A.H. Jawad, Box-Behnken design to optimize the synthesis of new crosslinked chitosan-glyoxal/TiO_2 nanocomposite: Methyl orange adsorption and mechanism studies, Int. J. Biol. Macromol., 129 (2019) 98–109.

[28] G. Karaçetin, S. Sivrikaya, M. Imamoğlu, Adsorption of methylene blue from aqueous solutions by activated carbon prepared from hazelnut husk using zinc chloride, J. Anal. Appl. Pyrolysis, 110 (2014) 270–276.

[29] K.E. Noll, 1991. Adsorption technology for air and water pollution control. CRC Press.